Table S1. Primer sequences used for genotyping.

Gene	Primer name	Sequence (5' – 3')
***Cxcl12*$^{\text{lacZ (3f)}}$**	Neo14	ctctatggcttctgaggcggaaag
	Cxcl12-GT4	cctgcagttgaccagtcgttcaga
***Cxcl12*$^{+/2f}$**	Cxcl12-GT3	aagatgatgagtttacgtttgaat
	Cxcl12-GT4	cctgcagttgaccagtcgttcaga
***Cxcl12*$^{+/1f}$**	Cxcl12-GT1	aaaactgcaggtggtagaagtgaa
	Cxcl12-GT4	cctgcagttgaccagtcgttcaga
Flpe	Flpe-F	gcaattacagttcgaatcatcgga
	Flpe-R	ccacaattgatgaaagtagctagg
Tg(*Tie2*-Cre)	Tie2-F1	acaagagcgagtggaccatgcgag
	IRESCre-R	atcaggttcttgcgaacctcatca

Table S2. Primer sequences used for RT-PCR and qRT-PCR analyses

		Primer name	Sequence (5'→3')
RT-PCR	*Cxcl12*	qCxcl12-F2	ATGGACGCCAAGGTCGTCGCC
		qCxcl12-R2	ACAATCTGAAGGGCACAGTTT
	Gapdh	Gapdh-F	ATGACCACAGTCCATGCCATCACT
		Gapdh-R	TCATACCAGGAAATGAGCTTGACA
qRT-PCR	*Cxcl12*	mCxcl12-Q-F1	TGCATCAGTGACGGTAAACCA
		mCxcl12-Q-R1	TTCTTCAGCCGTGCAACAATC
	Cyclophilin	mCyclo-Q3	TGCCGGAGTCGACAATGAT
		mCyclo-Q5	TGGAGAGCACCAAGACAGACA

Table S3: Genotypes of pups from *Cxcl12*$^{+/3f}$ crosses at weaning

	Cxcl12$^{+/+}$	*Cxcl12*$^{3f/+}$	*Cxcl12*$^{3f/3f}$	litter size
1	2	4	0	6
2	3	3	0	6
3	4	5	0	9
4	3	2	0	5
5	2	9	0	11
6	4	0	0	4
7	1	2	0	3
8	1	7	0	8
9	1	3	0	5
10	2	2	0	4
11	1	3	0	4
Total	24	40	0	65

Table S4: Genotypes of pups from timed-mating of *Cxcl12*$^{+/3f}$ mice

	Cxcl12$^{+/+}$	*Cxcl12*$^{+/3f}$	*Cxcl12*$^{3f/3f}$
E10.5	10	22	10
E11.5	2	9	5
E12.5	9	9	4
E13.5	8	17	11
E14.5	7	15	12
E15.5	8	21	11
E16.5	10	24	11
E17.5	20	41	17 (3)
E18.5	9	12	2 (2)

Numbers in parenthesis indicate the number of fetuses found dead

Table S5: Genotypes of pups from timed-mating of *Cxcl12*$^{+/1f}$ mice

	Cxcl12$^{+/+}$	*Cxcl12*$^{+/1f}$	*Cxcl12*$^{1f/1f}$
E10.5	6	13	5
E11.5	4	9	4
E12.5	4	8	3
E13.5	4	7	5
E14.5	10	19	9
E15.5	7	11	4
E16.5	12	24	13(1)
E17.5	22	57	25(10)
E18.5	7	15	7(2)
PN1	4	6	1 (1)

Numbers in parenthesis indicate the number of fetuses found dead

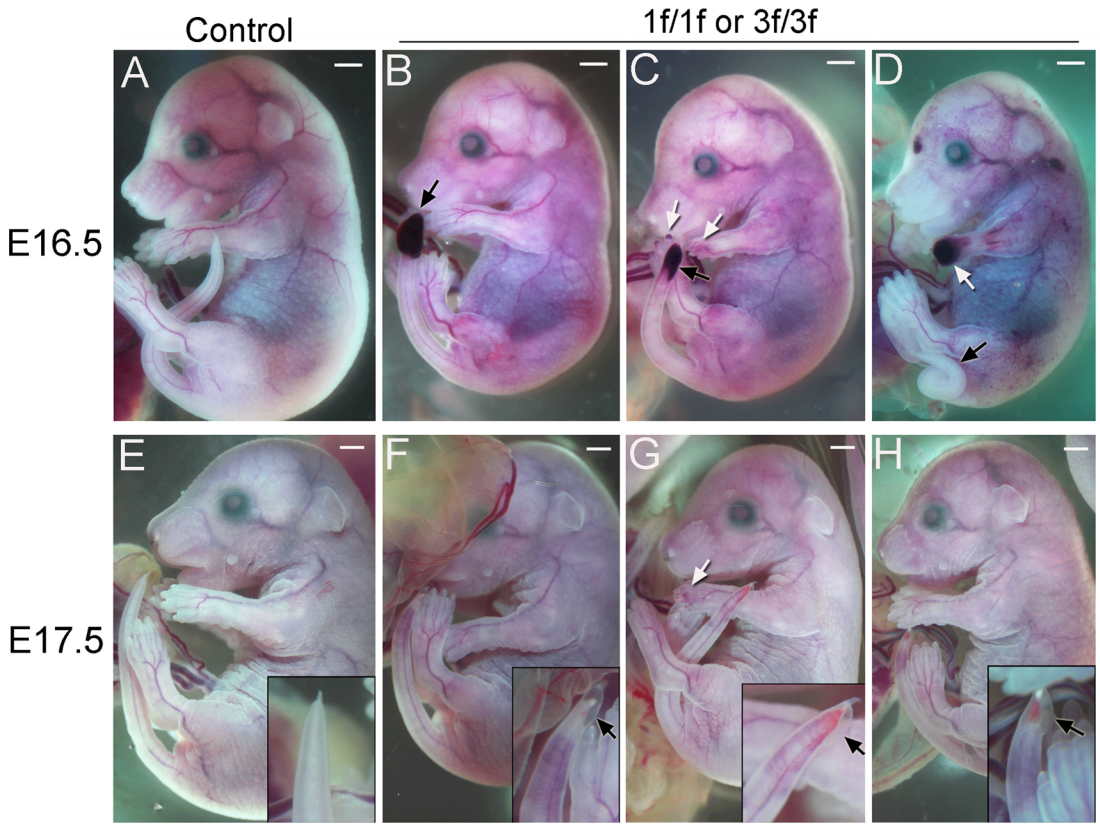

Figure S1. ***Cxcl12*-null mice exhibit defects in tails and limbs.**
Gross morphology of control (WT or heterozygotes; **A** and **E**, n>40 each) and *Cxcl12*-null fetuses at E16.5 (**B-D**, n>20) and E17.5 (**F-H**, n>30). The most consistent feature of *Cxcl12*-null mice is defects in the tail (black arrows) with hemorrhage (**B, C**), curl (**D**), kink, or edema (**F-H**). Some of them (~25%) showed hemorrhagic signs in the toes or paws (white arrows). Signs of hemorrhage in the skin were also observed in some cases, but it seemed to be associated with heart failure. Scale bars: A-H, 1 mm.

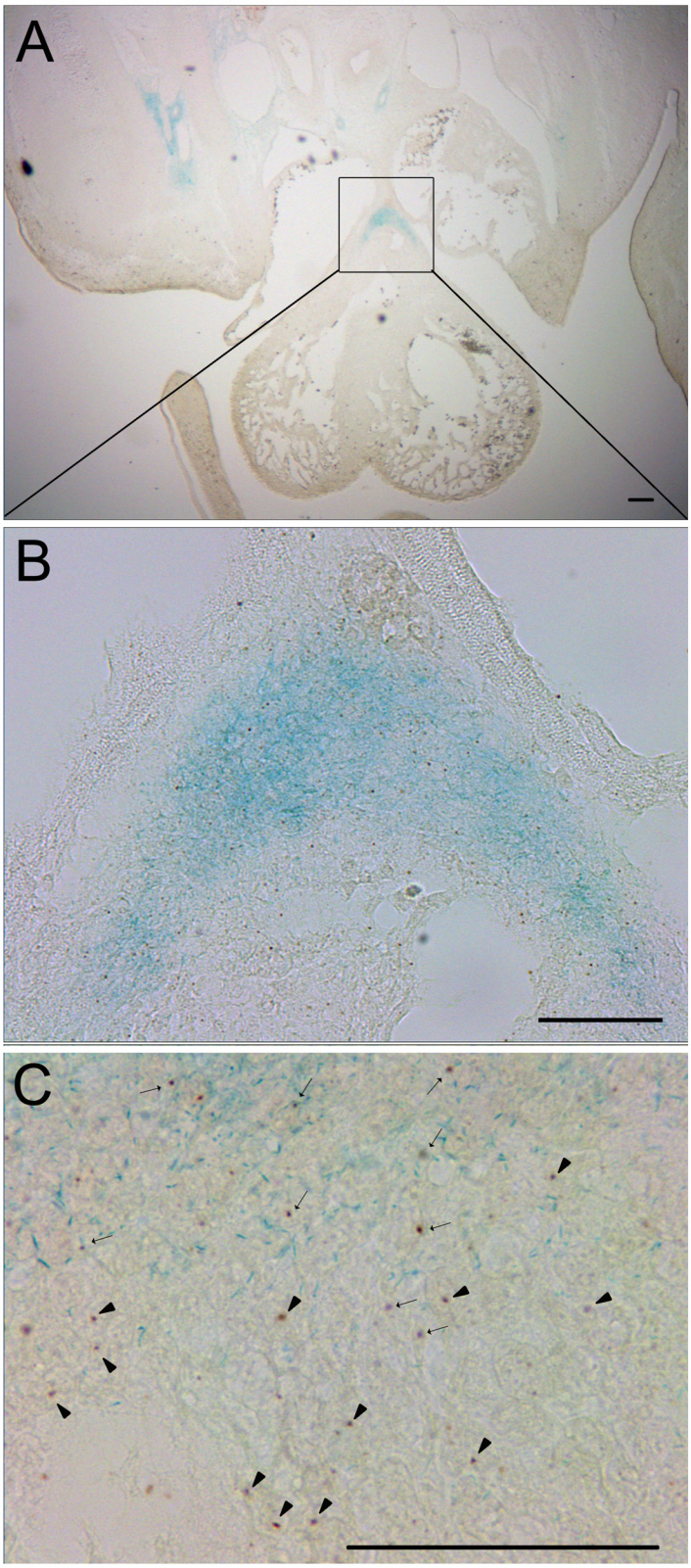

Figure S2. ***Isl1*** **expression in outflow tract of** ***Cxcl12***$^{+/3f}$ **embryo at E13.5:**
In situ hybridization of *Isl1* was performed on X-gal-stained section in the heart and outfow tract of E13.5 *Cxcl12*$^{+/3f}$ embryos. Isl1-expressing cells (small brown spots) and X-gal -positive cells (blue) were co-localized partially in the outflow tract of *Cxcl12*$^{+/3f}$ embryos. In panel C, arrows indicate cells positive for both *Isl1* and *Cxcl12*, and arrowheads mark cells negative for *Cxcl12* but positive for *Isl1* expression. Scale bar: A and B, 200 μm; C, 50 μm.

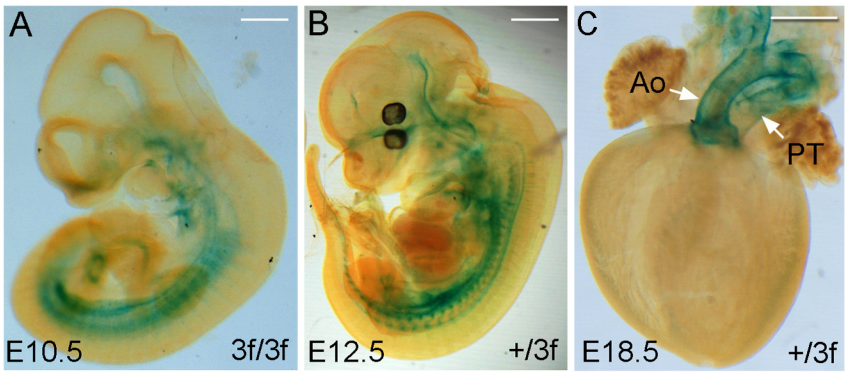

Figure S3. Expression of *Cxcl12* in developing embryos:
X-gal staining of *Cxcl12*$^{+/lacZ}$ (C*xcl12*$^{+/3f}$) embryos at E10.5 (A), E12.5 (B) and E18.5 (C). X-gal positive cells were found along the dorsal aorta and intersomitic vessels at E10.5 (**A**, n=5) and E12.5 (**B,** n=5). The aorta (Ao) and pulmonary trunk (PT) were X-gal positive (**C;** n>5). Scale bars: A, 500 µm; B-C, 1 mm

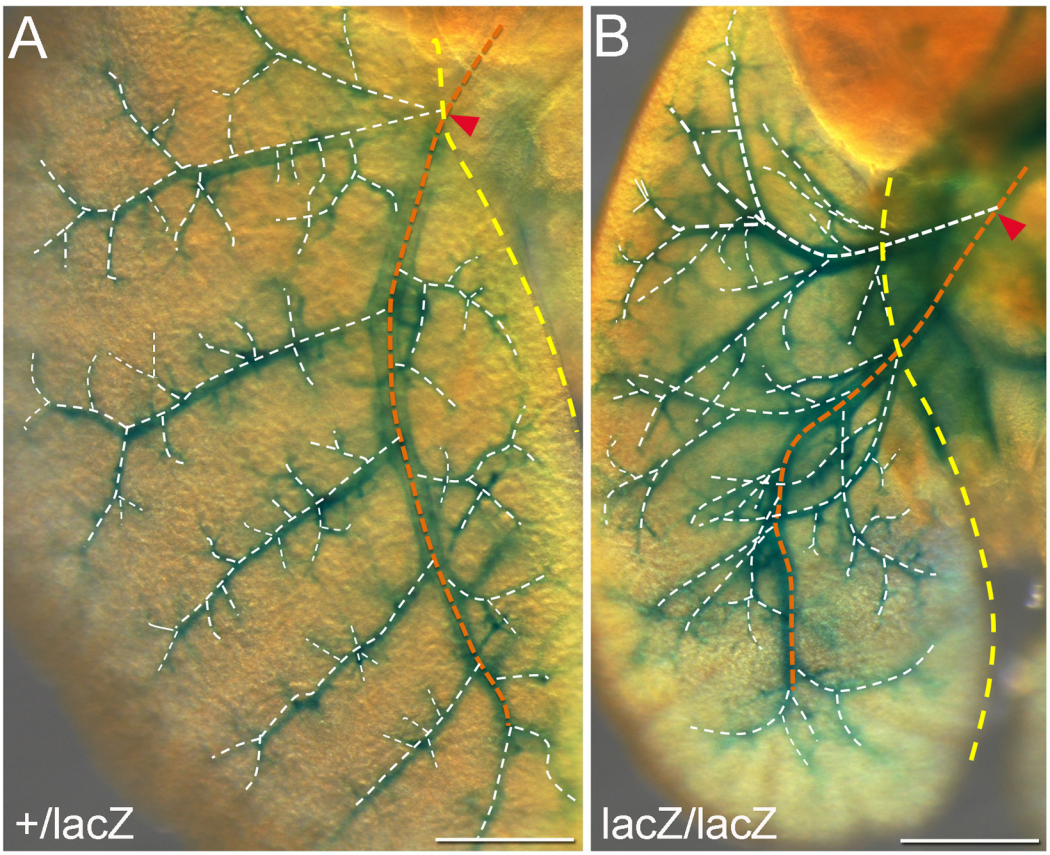

Figure S4. Disruption of the domain branching pattern of pulmonary arteries in *Cxcl12*-mutants. A and B. Tracing of PA branches visualized by X-gal staining in *Cxcl12*$^{+/3f}$ (**A**, n>5) and *Cxcl12*$^{3f/3f}$ (**B**, n>5) mice. PA branches from the common basal artery (orange dots) are regularly spaced and show the domain branching pattern in control lungs. However, PAs in the mutants are branched into two or more vessels without specific branching patterns. The first branching point (red arrowheads) from the common basal artery occurs as it enters into the lung parenchyma (yellow dots) in the controls (**A**), but the first branch appears in the more proximal regions before PA reaches to the lung (**B**). Scale bars: A-G, 500 μm.

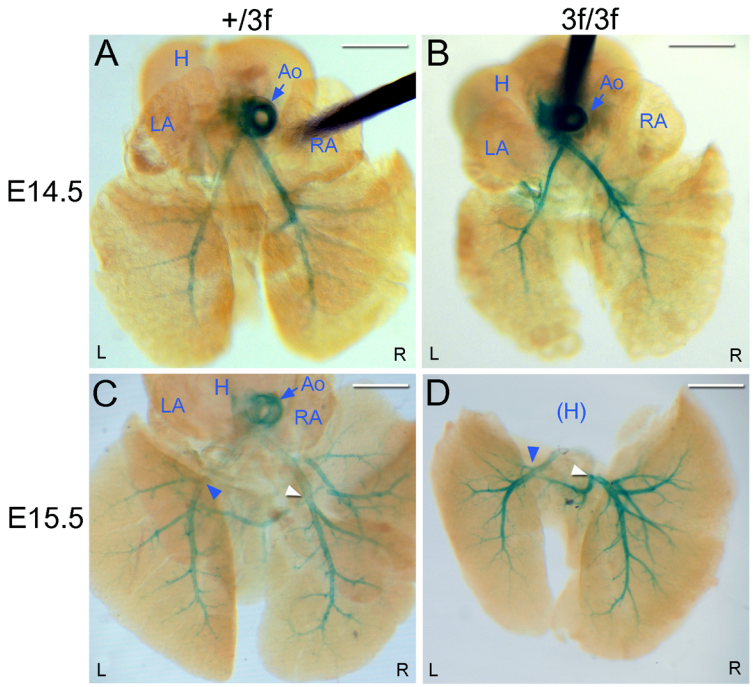

Figure S5. Aberrant PA branching patterns in *Cxcl12*-mutants at E14.5 and E15.5. Dorsal views of whole mount X-gal stained E14.5 (**A, B**; n>3) and E15.5 (**C, D**; n>3) control (*Cxcl12*$^{+/3f}$; **A, C**) and *Cxcl12*-null (*Cxcl12*$^{3f/3f}$; **B, D**) hearts and lungs. The heart of E15.5 mutant (**D**) was removed for better visualization. In the control embryos, arteries branch off from the basal arteries in a regularly spaced domain branching pattern, whereas the branching patterns in the mutants are irregular and mostly follow a bifurcation branching pattern. Branching points to the accessory lobe from the right basal artery (white arrowheads) and apical/anterior arteries from the left basal artery (blue arrowheads) occurs at more proximal sites in the mutants. Ao: aorta, H: heart, LA: left atrium, RA: right atrium. Scale bar: A-D, 500 µm.

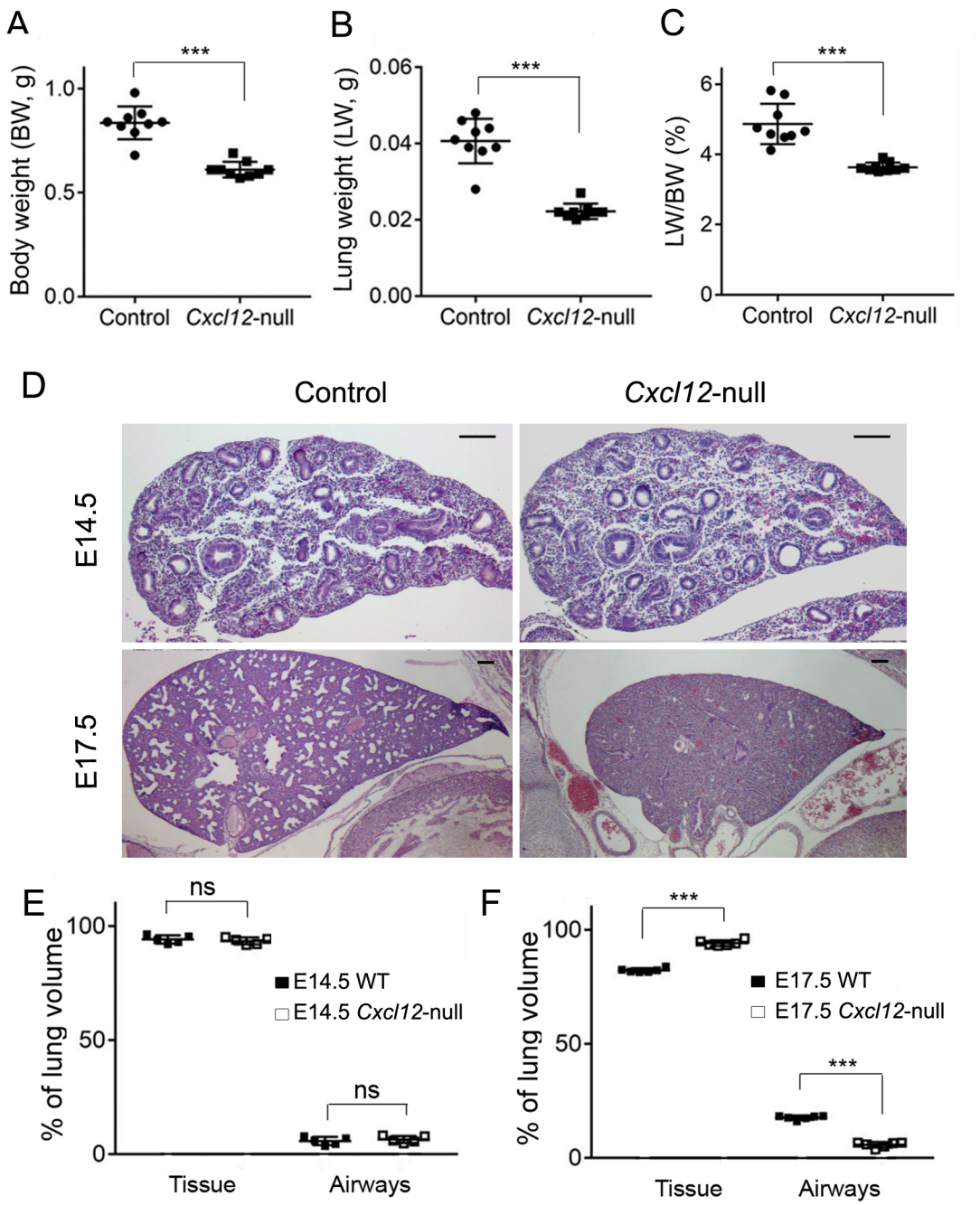

Figure S6. Impaired growth and maturation of the Cxcl12-mutant lungs at late gestation periods: The weights of whole body (**A**) and the lungs (**B**) of E17.5 *Cxcl12*-null embryos (n=9) were reduced compared with those in the littermate controls (n=9). The ratio of lung weight to body weight (**C**) was also lower in the mutants than controls. ***P<0.0001. **D.** H&E stained sections of E14.5 and E17.5 control and *Cxcl12*-null left lungs (n=5 for each genotype and stage). Scale bars in the E14.5 section indicate 100 μm; in the E17.5 section 200 μm. **E and F.** Percentages of areas of tissue (cells and matrix) and airway space in the sections of *Cxcl12*-mutants at E14.5 nd E17.5 were compared with those of controls. While no difference was observed in E14.5 lungs (**E**), the percentages of tissue and airway areas of mutants were increased and decreased, respectively, in E17.5 lungs compared with those of controls (F). ***P<0.0001.

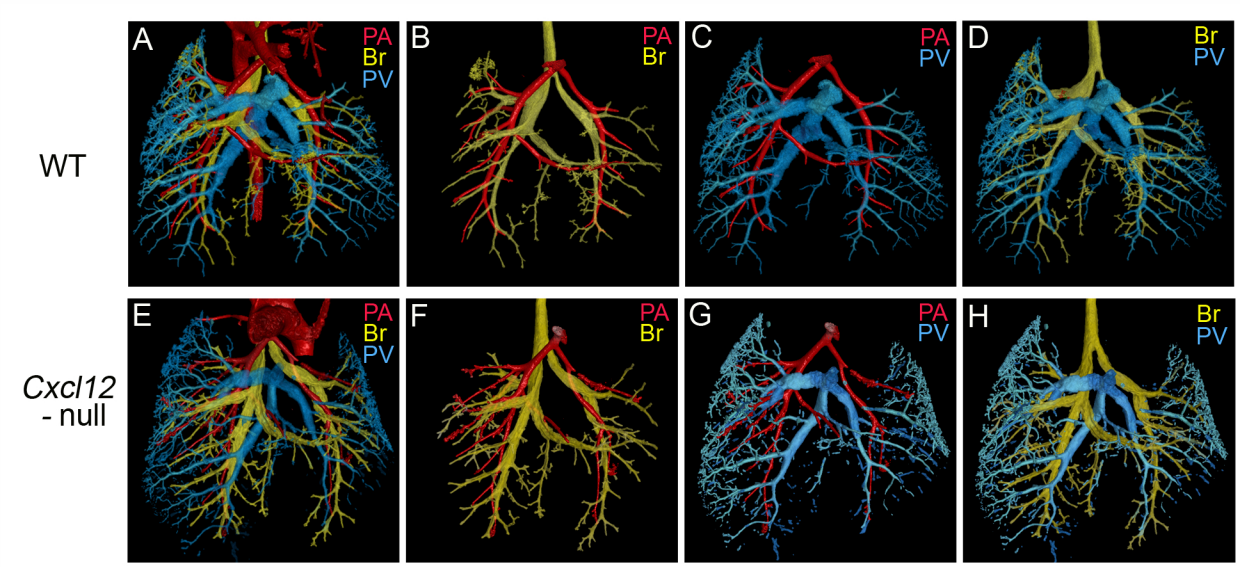

Figure S7. Misalignment of pulmonary arteries with normal pulmonary veins and bronchial branches in the *Cxcl12*-null lungs: Frontal views of color-coded diceCT images of pulmonary artery (PA, red), pulmonary vein (PV, blue) and bronchial tree (Br, yellow) of E17.5 wild-type (**A**-**D**) and *Cxcl12*-null (**E**-**H**) embryos. In WT lungs, PA, PV, and Br are parallel to one another. In *Cxcl12*-null lungs, however, PAs are discoordinated with PV and Br, while PV and Br are aligned as they are in the control lungs.

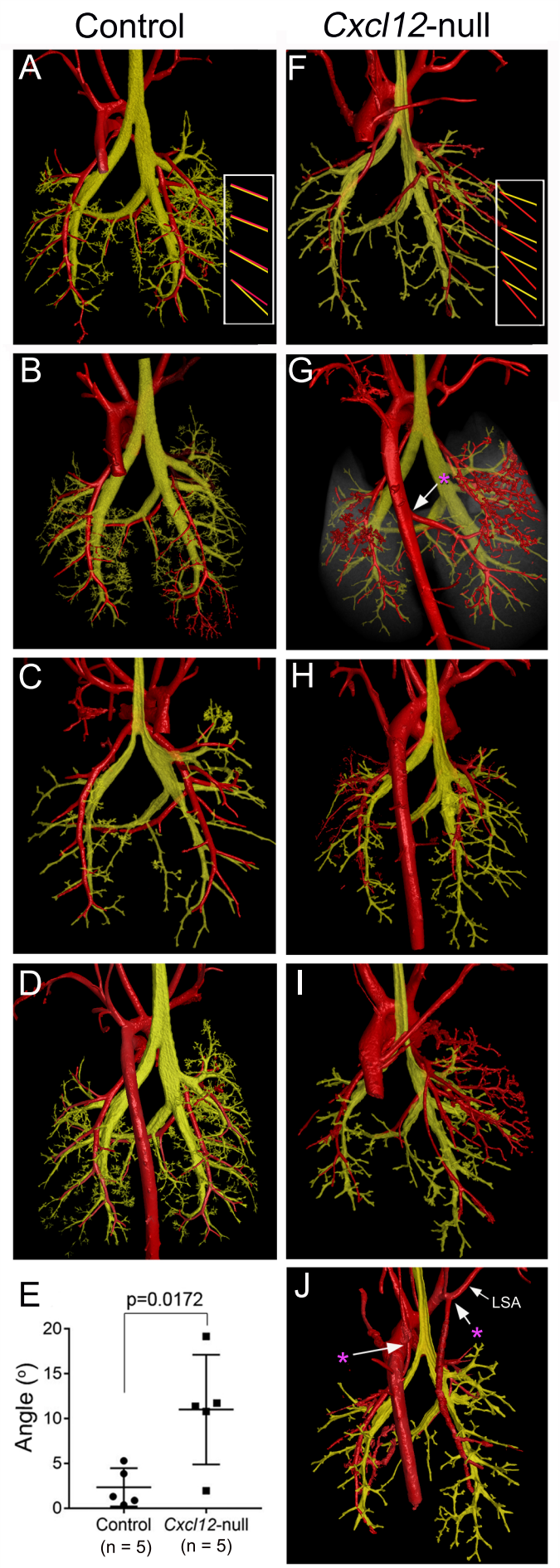

Figure S8. Misalignment of pulmonary arteries with bronchial branches in the *Cxcl12*-null lungs: Dorsal views of systemic and pulmonary arteries (red) and bronchial trees (yellow) of E17.5 wild-type (**A**-**D**) and *Cxcl12*-null (**F**-**J**) embryos. **E.** The angles between neighboring PAs and airways in the mutant (**F**) are wider than those in controls (**A**), indicating the misalignment of arteries and airways (Control: total 86 branches in 5 lungs; *Cxcl12*-null: total 77 branches in 5 lungs). *P=0.017. Abnormal systemic arterial supplies to lungs were indicated by arrows in **G** and I.